Electronic supplementary information (ESI)

A Single-Molecule Magnet Assembly Exhibiting Dielectric Transition below 470 K

Yu-Xia Wang,[a] Wei Shi,[a,*] Han Li,[a] You Song,[b] Liang Fang,[c] Yanhua Lan,[d,*] Annie K. Powell,[d] Wolfgang Wernsdorfer,[e] Liviu Ungur,[f] Liviu F. Chibotaru,[f,*] Mingrong Shen,[c] and Peng Cheng[a,*]

[a]*Department of chemistry and Key Laboratory of Advanced Energy Materials Chemistry (MOE), Nankai University, Tianjin 30071, P.R. China, E-mail: shiwei@nankai.edu.cn; pcheng@nankai.edu.cn*
[b]*State Key Laboratory of Coordination Chemistry, Nanjing National Laboratory of Microstructures, School of Chemistry and Chemical Engineering Nanjing University, Nanjing 210093, P. R. China.*
[c]*Department of Physics and Jiangsu Key Laboratory of Thin Films, Soochow University, Suzhou 215006, P. R. China.*
[d]*Institute of Inorganic Chemistry, Karlsruhe Institute of Technology, Engesserstrasse 15, 76131 Karlsruhe, Germany, E-mail: yanhua.lan@kit.edu*
[e]*Institut Néel—CNRS, BP 166, 25 Avenue des Martyrs, 38042 Grenoble Cedex 9, France.*
[f]*Division of Quantum and Physical Chemistry, Katholieke Universiteit Leuven, Celestijnenlaan 200F, B-3001, Heverlee, Belgium, Liviu.Chibotaru@chem.kuleuven.be*

1. Materials and methods, crystallographic study, computational details of the *ab initio* calculations

Materials and methods: All reagents were commercially available and used without further purification. Elemental analyses (C, H and N) were performed on a Perkin-Elmer 240 CHN elemental analyzer. IR spectra were recorded in the range of 400-4000 cm^{-1} on a Bruker TENOR 27 spectrophotometer using a KBr pellet. Powder X-ray diffraction measurements were recorded on a D/Max-2500 X-ray diffractometer using Cu-Kα radiation. Thermogravimetric analysis (atmosphere) was carried out in a Rigaku PTC-10ATG-DTA analyzer. DSC was performed by a Netzsch DSC 204 F1 analyzer (nitrogen atmosphere). Ferroelectric measurements were performed on a single crystal using the Radiant Technologies Premier Precision II ferroelectric tester. The temperature dependence of permittivity and dielectric loss were measured on a wafer (diameter ~ 10 mm, thickness ~ 1 mm) of polycrystalline powder sample using a Precision LCR Meter (HP 4284A) with frequency of 100 Hz to 1 MHz. Magnetic measurements were measured on microcrystalline samples using a Quantum Design MPMS XL-7 SQUID magnetometer. The magnetic data were corrected for the diamagnetic contribution of both the sample holder and the diamagnetic correction estimated using Pascal's constants.

Crystallographic study: Diffraction intensity data for single crystals of **Dy_3L** was collected at 120 – 463 K on an Oxford SuperNova diffractometer equipped with graphitemonochromated Mo-*K*α radiation (λ = 0.71073 Å). The structures were solved by the direct method and refined by the full-matrix least-squares method on F^2 with anisotropic thermal parameters for all non-hydrogen atoms.[1] Hydrogen atoms were located geometrically and refined isotropically. See Table S1 for details.

Computational details of the *ab initio* calculations: The calculations were done for mononuclear Dy^{III} fragments with the MOLCAS-7.6 quantum chemistry package and their local magnetic properties have been calculated with the module SINGLE_ANISO.[2] On the basis of these calculations, the exchange spectrum and the magnetic properties of

Dy_3L have been simulated within the Lines model using the program POLY_ANISO. This ab initio methodology is described elsewhere in detail.[3,4] All employed basis sets were taken from the standard ANO-RCC basis set library from MOLCAS. The following contractions were used for the atoms:

Dy – 8s7p5d4f2g1h

La –7s6p4d3f1g.

N, O – 4s3p2d1f. (Only for the first coordinated atoms, which make a bond with Dy)

N,O, C – 3s2p. (for distant atoms)

H – 2s.

Active space of the CASSCF method included 9 electrons in 7 orbitals. The spin orbit interaction was computed by mixing of 21 sextets, 128 quartets and 32 doublets spin free states. The results are given in the text, Tables S2-S6, and Figures S3-S5.

a) b)

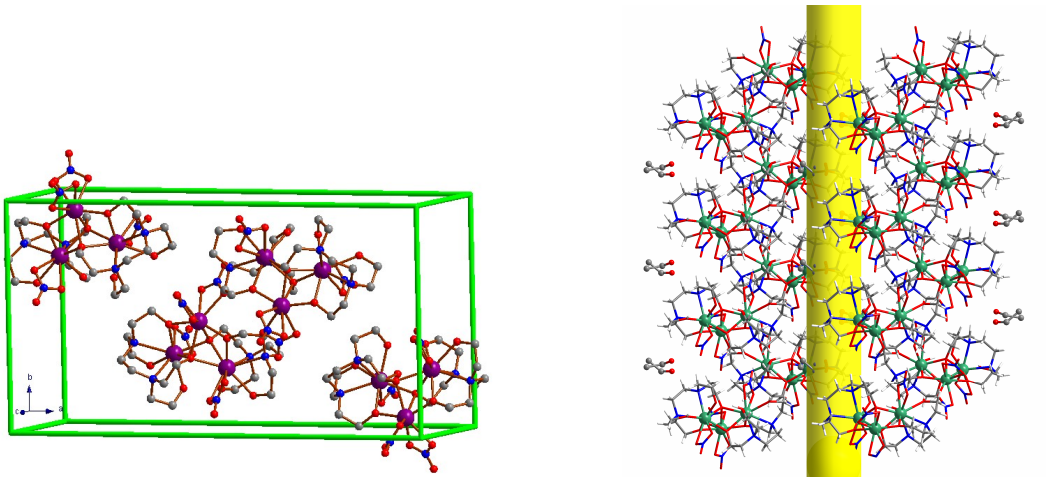

Fig. S1 a) The four different orientation **Dy_3L** molecules in a unit cell; b) The trinuclear units and ethanol surround the 2_1 screw axis (highlighted as yellow column).

Table S1 Single crystal parameters of **Dy_3L** at different temperatures.

	1	**2**	**3**	**4**	**5**
formula	$C_{22}H_{49}Dy3N_8O_{21}$	$C_{22}H_{49}Dy3N_8O_{21}$	$C_{22}H_{49}Dy3N_8O_{21}$	$C_{22}H_{49}Dy3N_8O_{21}$	$C_{22}H_{49}Dy3N_8O_{21}$
fw	1249.19	1249.19	1249.19	1249.19	1249.19
temp(K)	120(2)	200(2)	293(2)	373(2)	463(2)
crystal system	Orthorhombic	Orthorhombic	Orthorhombic	Orthorhombic	Orthorhombic
space group	$Pna2_1$	$Pna2_1$	$Pna2_1$	$Pna2_1$	$Pna2_1$
a (Å)	28.1795(7)	28.1693(7)	28.2865(11)	28.4138(6)	28.5392(19)
b (Å)	14.8684(4)	14.8554(4)	14.8604(8)	14.9179(3)	14.9764(6)
c (Å)	8.9668(2)	9.0020(3)	9.0607(6)	9.1126(2)	9.1530(4)
α (deg)	90	90	90	90	90
β (deg)	90	90	90	90	90
γ (deg)	90	90	90	90	90
V (Å^3)	3756.93(16)	3767.03(19)	3808.7(3)	3862.60(14)	3912.1(3)
Z	4	4	4	4	4
Dc (g·cm^{-3})	2.198	2.203	2.179	2.148	2.118
μ (mm^{-1})	5.996	5.981	5.915	5.833	5.759
R_{int}	0.0225	0.0273	0.0243	0.0249	0.0264
GOF	1.058	1.033	1.047	1.068	1.060
R1	0.0404	0.0400	0.0385	0.0277	0.0324
wR2	0.0986	0.0970	0.0947	0.0579	0.0740
$\triangle\rho_{max}$ (e Å^{-3})	2.281	1.270	0.975	0.624	0.531
$\triangle\rho_{min}$ (eÅ^{-3})	-1.766	-0.837	-1.046	-0.524	-0.826
flack	0.007(19)	-0.016(17)	-0.006(19)	-0.014(13)	-0.033(17)

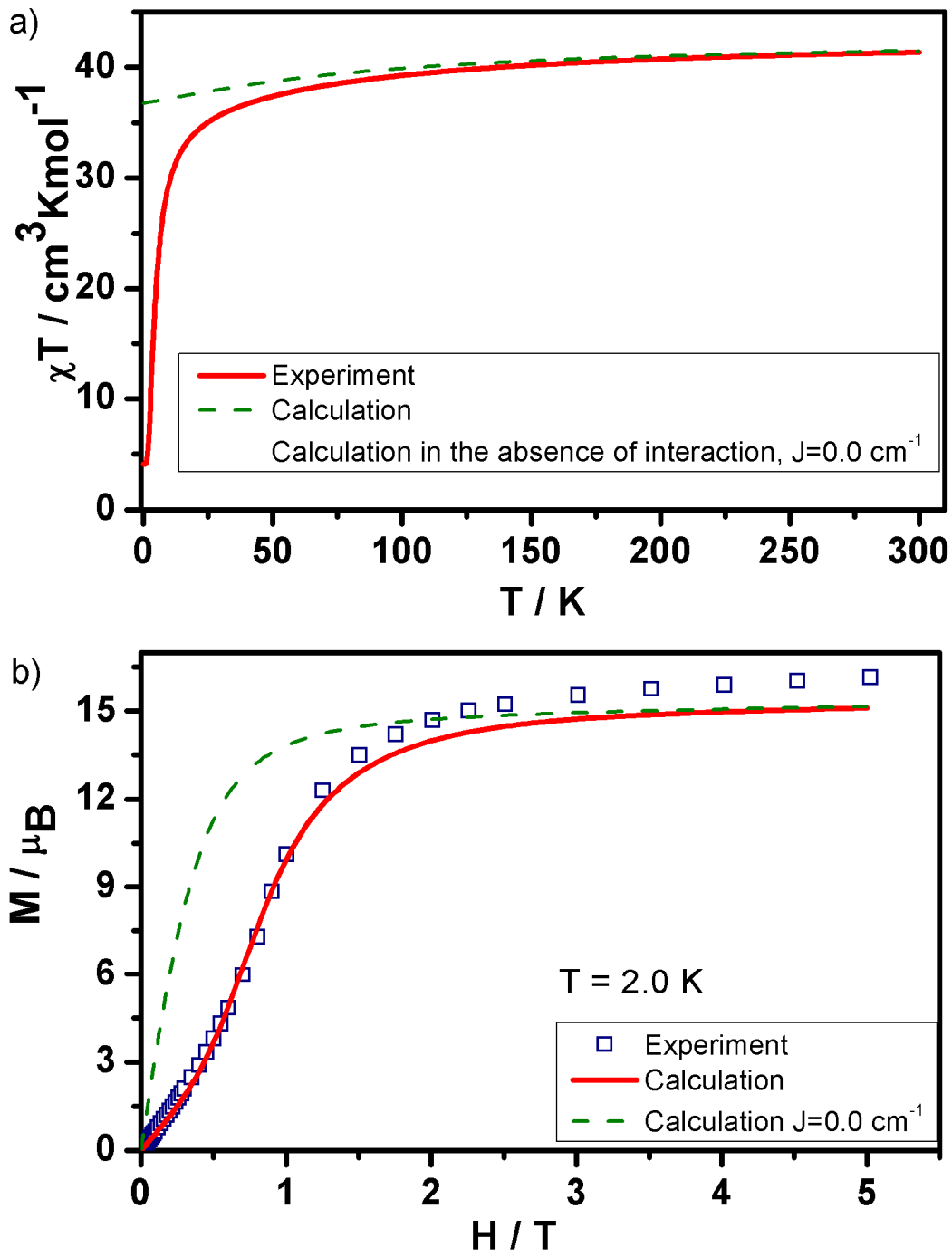

Fig. S2 A comparison between measured (empty squares) and calculated (red line) magnetic data. a) Magnetic susceptibility and b) molar magnetization at 2.0 K for **Dy_3L**. Dashed green lines show the calculated magnetic properties in the absence of any magnetic interaction between Dy centers.

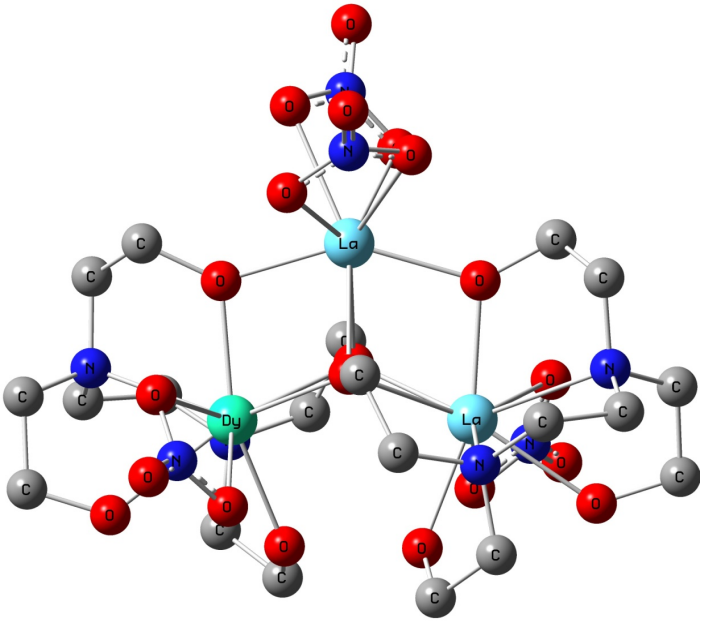

Fig. S3 Structure of the calculated Dy1 fragment of the **Dy_3L** complex. Model fragments for Dy2 and Dy3 are similar. Hydrogen atoms are not shown for clarity.

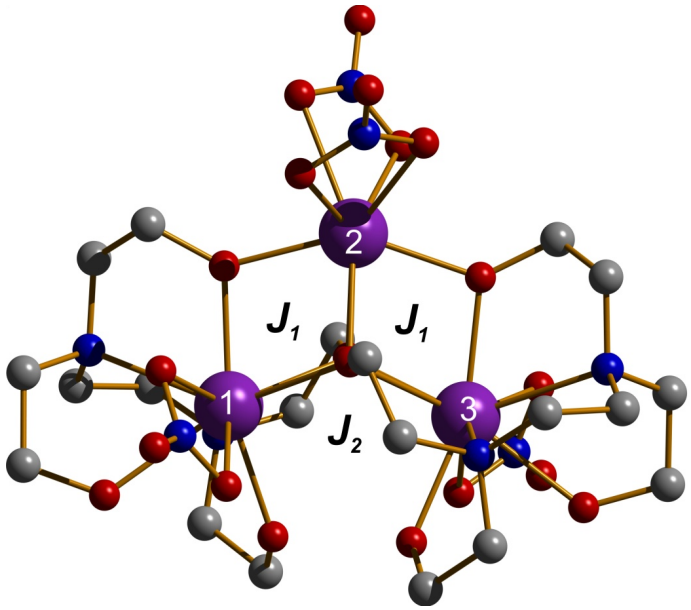

Fig. S4 The numbering of the magnetic centers and corresponding exchange interactions considered for **Dy_3L**. Due to the structural differences, two exchange parameters were employed: Dy1 — Dy2 and Dy2 — Dy3 were simulated by Lines parameter J_1. Dy1 — Dy3: was simulated by Lines parameter J_2.

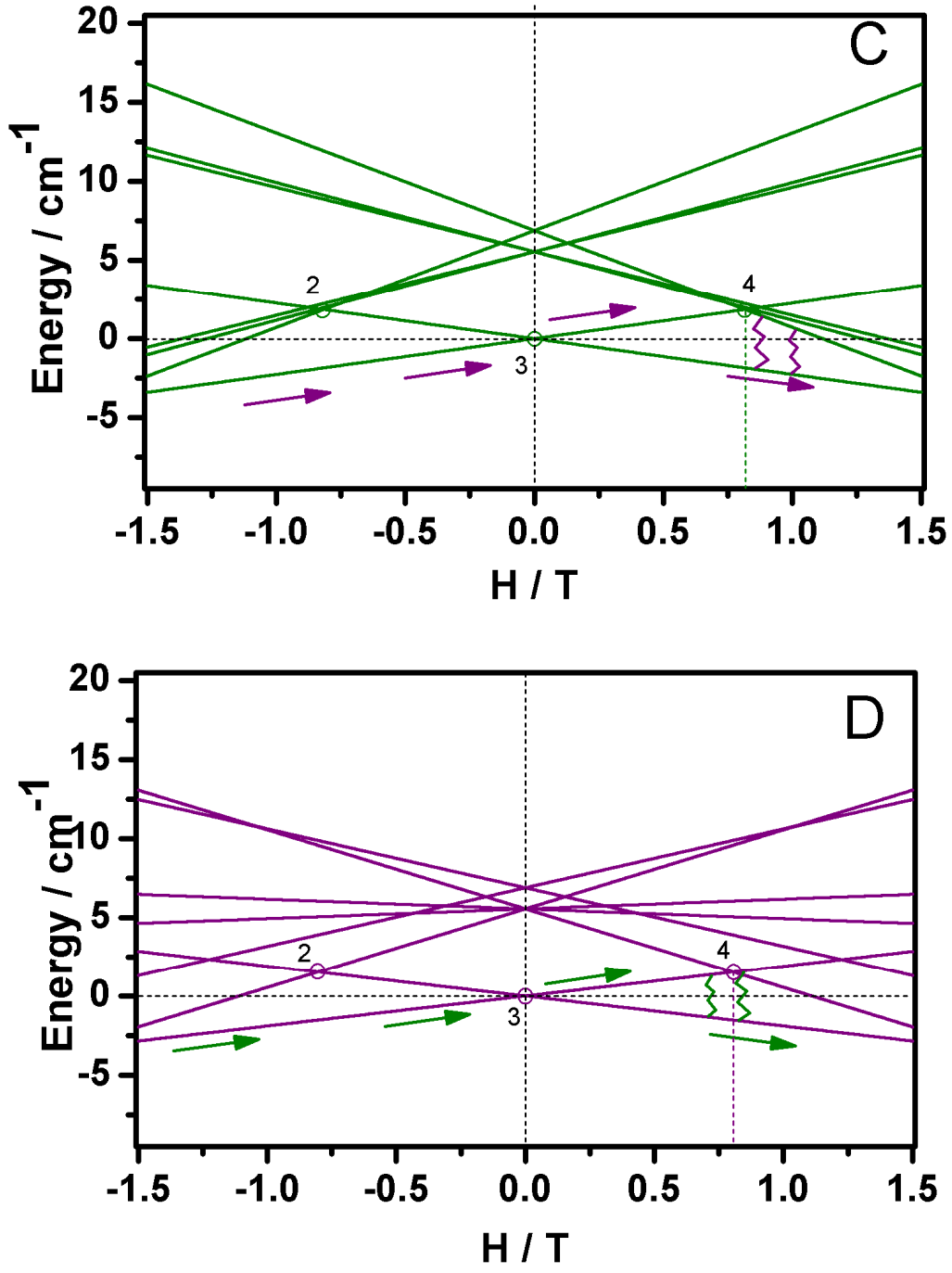

Fig. S5 Energy levels of molecules **Dy_3L**-C and **Dy_3L**-D in applied magnetic field. Wiggly lines show relaxation transition from higher to lower levels.

Table S2 CASSCF energies of the lowest spin-free states (cm^{-1}) on magnetic sites.

Spin multiplicity		**Spin free energies**		
		Dy1	**Dy2**	**Dy3**
	H	0.000 7.105 127.097 193.083 247.455 275.445 368.882 521.716 577.320 626.592 659.052	0.000 20.433 356.451 398.607 567.180 578.888 675.304 694.458 745.495 1050.152 1061.231	0.000 9.632 327.296 358.185 585.232 669.806 699.659 786.864 904.851 934.775 970.246
	F	7579.917 7726.934 7782.864 7833.251 7843.669 7858.103 7904.113	7801.507 7926.977 7952.199 8018.801 8121.462 8162.868 8205.577	7766.876 7977.230 8026.572 8071.946 8126.272 8135.237 8197.626
	P	34822.825 35084.226 35351.213	34742.966 35405.948 35775.214	34746.633 35597.504 35672.682
4		24856.889 24860.846 24952.307 24974.145 24983.408 25025.233 25039.994 25066.395 25074.609 25092.708 25100.643 25163.324 25179.510 25245.026 25249.155 25267.934 25320.043 25333.683 25351.292 25370.442 …	24974.791 24978.840 25193.108 25220.969 25237.439 25251.581 25263.507 25290.265 25314.292 25332.586 25351.928 25379.107 25396.104 25442.767 25449.930 25496.819 25507.934 25531.385 25568.558 25580.165 …	24949.095 24951.317 25165.185 25205.876 25211.802 25258.125 25276.222 25279.868 25308.217 25344.680 25362.287 25405.711 25426.561 25440.255 25466.479 25474.197 25546.977 25558.796 25579.060 25633.566 …
2		37297.898 37298.393 37388.030 37406.603 37434.037 37476.160 37495.494	37523.784 37524.986 37602.051 37613.213 37634.898 37650.328 37726.688	37480.576 37480.679 37630.968 37653.962 37676.831 37732.925 37750.658

		37509.364	37771.229	37763.850
		37566.204	37796.731	37800.918
		37568.995	37819.825	37816.061
		37595.468	37824.699	37838.787
		37632.117	37845.358	37865.179
		37641.489	37873.773	37874.245
		37691.034	37880.464	37906.186
		37701.204	37902.588	37928.337
		37711.746	37919.680	37965.977
		37736.527	37939.768	37989.825
		39014.405	39181.982	39188.254
		39017.386	39185.779	39189.450
		39117.190	39321.983	39381.607
		…	…	…

Table S3 Energies of the lowest spin-orbit states (cm^{-1}).

Spin-orbit energies		
Dy1	**Dy2**	**Dy3**
0.000	0.000	0.000
108.778	239.577	225.784
202.571	459.170	485.721
286.735	546.174	634.670
322.050	587.706	672.382
385.913	642.290	711.704
458.087	709.691	753.551
524.465	979.880	834.336
3588.382	3655.154	3647.840
3750.963	3891.903	3943.661
3786.642	3997.455	4042.065
3817.530	4067.116	4104.722
3862.539	4113.709	4185.441
3920.620	4209.170	4250.042
3969.606	4377.185	4292.988
6179.705	6305.915	6305.334
6258.538	6446.123	6476.664
6306.161	6530.159	6525.643
6327.785	6605.982	6614.644
6398.042	6720.221	6732.125
6501.819	6865.604	6832.322
8148.655	8311.754	8323.897
8203.472	8413.444	8425.359
8262.383	8501.166	8511.458
8321.665	8615.075	8607.328
8444.220	8783.313	8774.151
9664.689	9857.271	9860.109
9752.818	9978.550	9994.902
9816.033	10085.800	10058.946
9956.448	10279.513	10273.587
10076.755	10300.307	10317.011
10133.493	10320.571	10350.076
10169.281	10404.692	10411.842

10189.886	10457.754	10502.775
10247.612	10514.488	10525.619
10267.475	10557.554	10585.768
10828.479	11024.838	11005.472
10999.896	11294.024	11325.236
11096.305	11541.031	11413.387
11553.865	11833.913	11817.418
11578.611	11893.110	11842.429
11614.188	11914.242	11866.267
11630.477	11945.674	11909.531
11652.239	11991.528	11950.530
13469.071	13747.434	13731.284
13533.770	13796.479	13802.564
13557.196	13846.655	13829.761
13582.789	13878.109	13864.110
14943.960	15217.196	15202.186
14987.229	15274.297	15265.946
15014.904	15305.250	15291.240
15842.607	16177.233	16116.439
15851.967	16201.608	16124.077
16377.550	16696.767	16654.967
24610.941	25201.739	24851.043
24674.565	25438.510	24913.194
24695.427	25466.373	24949.128
24771.960	25490.504	24993.019
24914.564	25529.037	25153.488
25098.119	25579.378	25181.448
25297.352	25606.981	25570.862
25344.616	25671.319	25631.514
25366.465	25709.657	25641.551
25392.533	25794.608	25655.881
25424.959	25836.848	25696.432
25451.495	25913.344	25751.939
25495.810	25995.623	25795.300
27322.137	27928.740	27450.848
27336.705	28040.273	27529.967
27398.519	28163.085	27669.163
27438.021	28222.806	27718.802
27460.992	28276.847	27755.235
27527.426	28346.703	27811.884
27592.358	28773.447	27842.053
27645.750	28807.437	27853.065
…	…	…

Table S4 Exchange energies (cm^{-1}) and main values of the *g* tensor for the 4 lowest exchange Kramers doublets.

ID	**Energy (cm^{-1})**	Main values of the g-tensor	
1	0.000000000	g_X	0.00000000000000
	0.000000000	g_Y	0.00000000000000

		g_Z	11.45644757987305
2	5.544265849 5.544265849	g_X	0.00000321148244
		g_Y	0.00142614450981
		g_Z	43.19580620798816
3	5.549332356 5.549332356	g_X	0.00000324344092
		g_Y	0.00142327953888
		g_Z	43.39263132310562
4	6.886124785 6.886124785	g_X	0.00000010000000
		g_Y	0.00000034653691
		g_Z	28.25836813821110

Note: The main anisotropy axis of the total complex, i.e. the g_z axis for the first exchange Kramers doublet makes an angle of 7.93° with the plane of **Dy_3L**.

Table S5 Tunneling gaps (cm^{-1}) of level crossings for all four **Dy_3L** molecules from a unit cell for the chosen direction of the applied magnetic field. (See Fig. 2, inset from the main text and Fig. S5).

Point	**Dy_3L-A**	**Dy_3L-B**	**Dy_3L-C**	**Dy_3L-D**
1	0.113931E-01 H = -0.947260 T	0.555193E-04 H = -0.710452 T	0.369519E-04 H = -1.763734 T	0.182884E-02 H = -1.788086 T
2	0.747410E-07 H = -0.531131 T	0.250425E-05 H = -0.480347 T	0.282730E-03 H = -0.816246 T	0.266156E-05 H = -0.804199 T
3	0.000 H = 0.000 T	0.000 H = 0.000 T	0.000 H = 0.000 T	0.000 H = 0.000 T
4	0.747410E-07 H = 0.531131 T	0.250425E-05 H = 0.480347 T	0.282730E-03 H = 0.816246 T	0.266156E-05 H = 0.804199 T
5	0.113931E-01 H = 0.947260 T	0.555193E-04 H = 0.710452 T	0.369519E-04 H = 1.763734 T	0.182884E-02 H = 1.788086 T
6	0.662146E-03 H = 0.914404 T	---	---	---

2. Magnetic properties

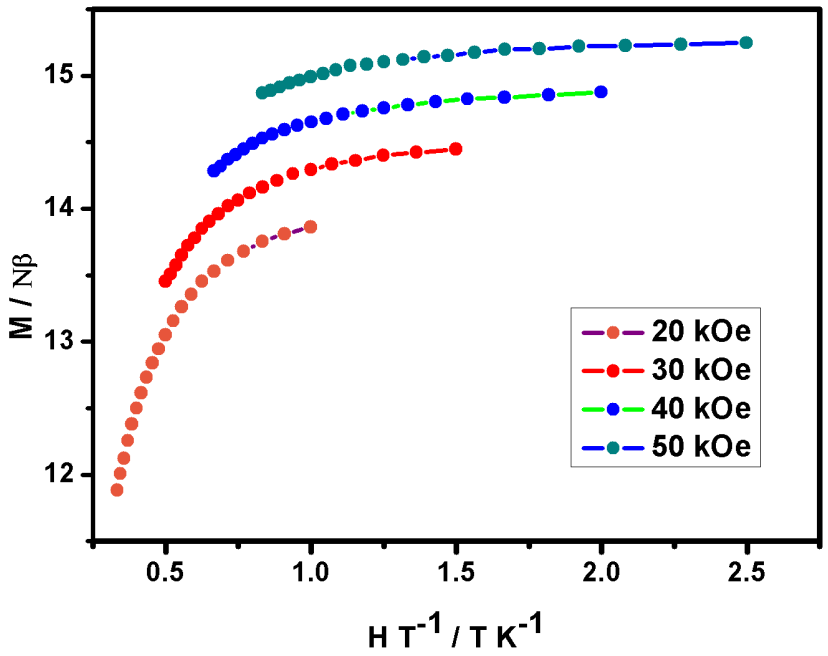

Fig. S6 Magnetization (*M*) *vs. H*/*T* plots of **Dy_3L** measured at different fields. Solid lines are eye guides.

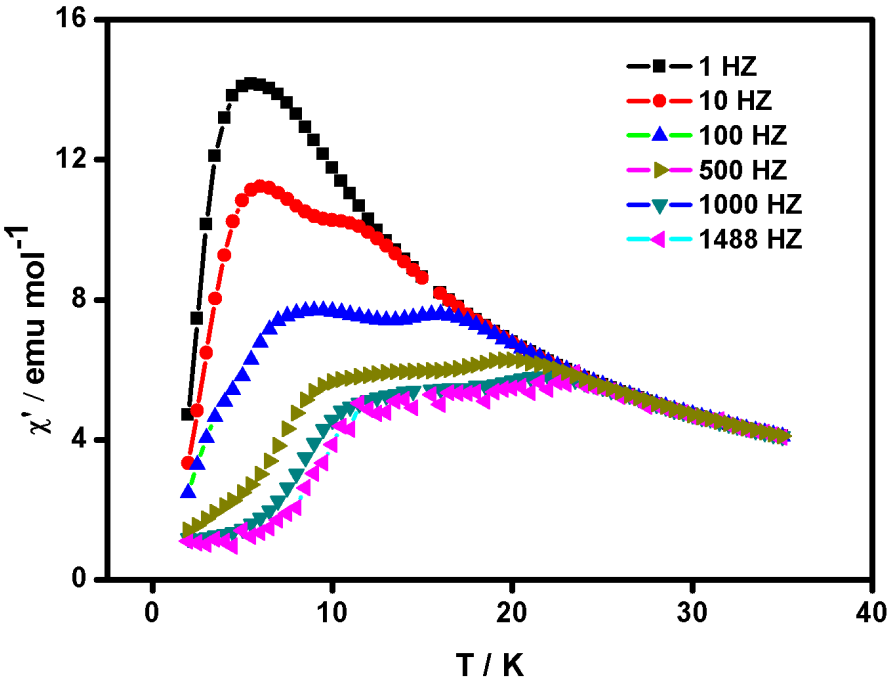

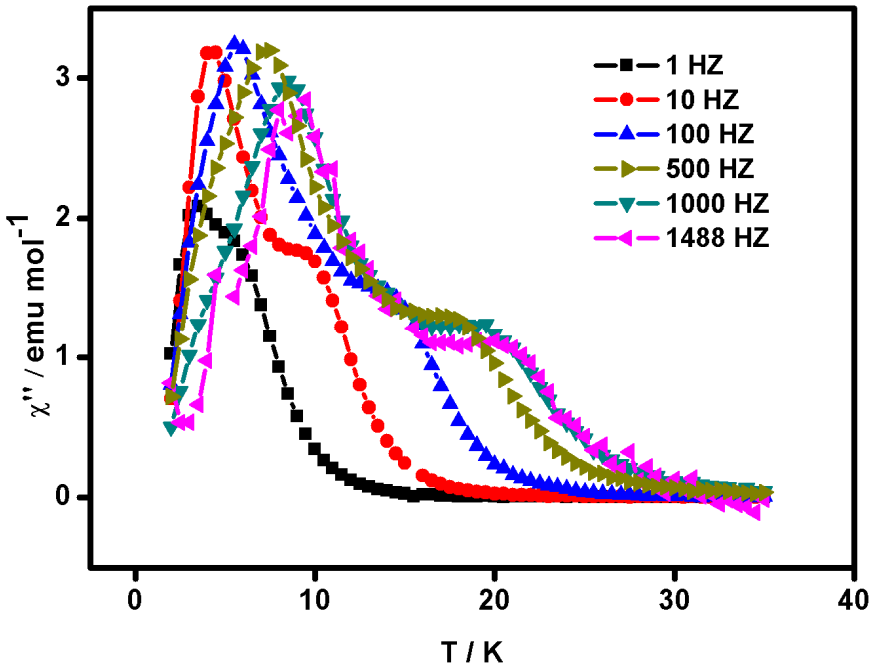

Fig. S7 Temperature dependence of the in-phase (χ') and out-of-phase (χ'') ac susceptibilities measured on a polycrystalline sample in the zero static filed. Solid lines are eye guides.

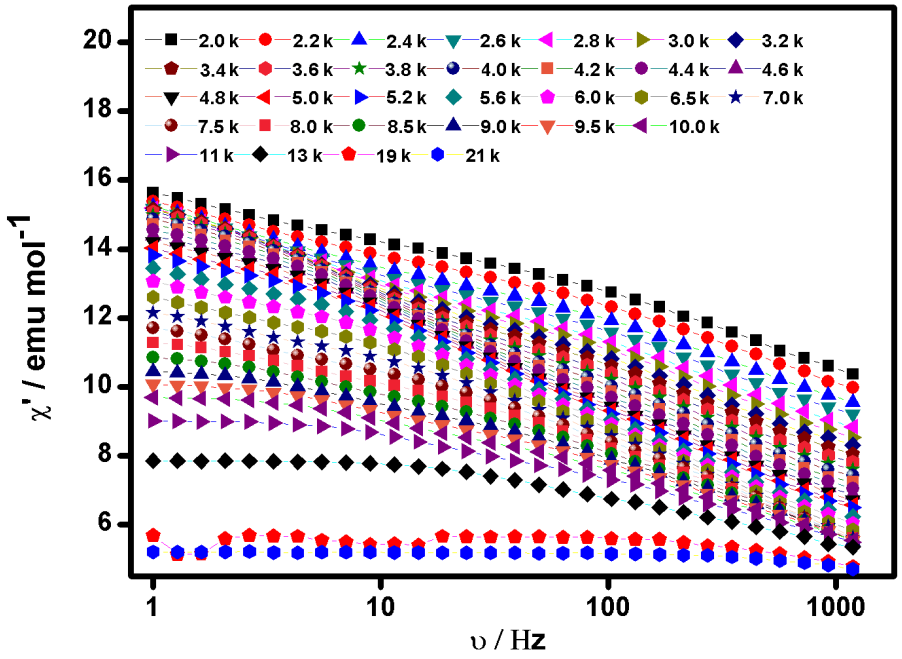

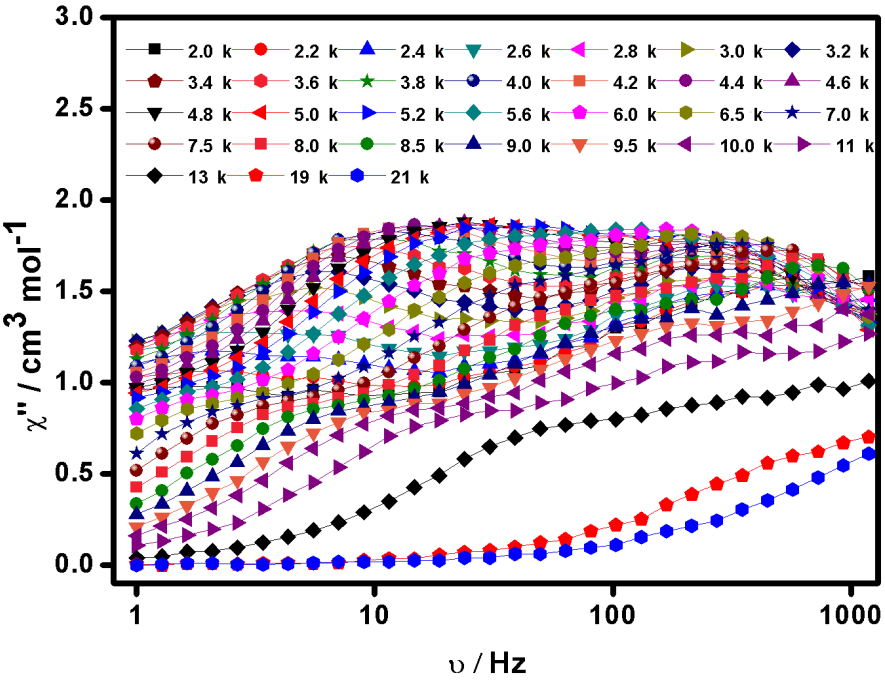

Fig. S8 Frequency dependence of the in-phase (χ') and out-of-phase (χ'') ac susceptibilities measured on a polycrystalline sample in the zero static filed. Solid lines are eye guides.

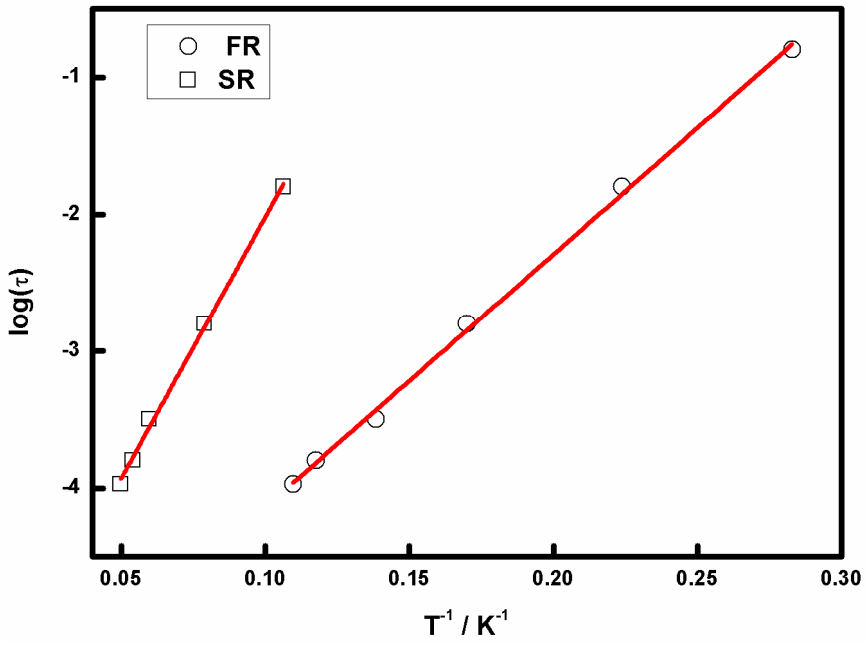

Fig. S9 The log (τ) (fast relaxation phase, FR) and log (τ_2) (slow relaxation phase, SR) verse T^{-1}, τ_1 and τ_2 are relaxation times of the fast phase and slow phase, respectively. The red lines are the best fits.

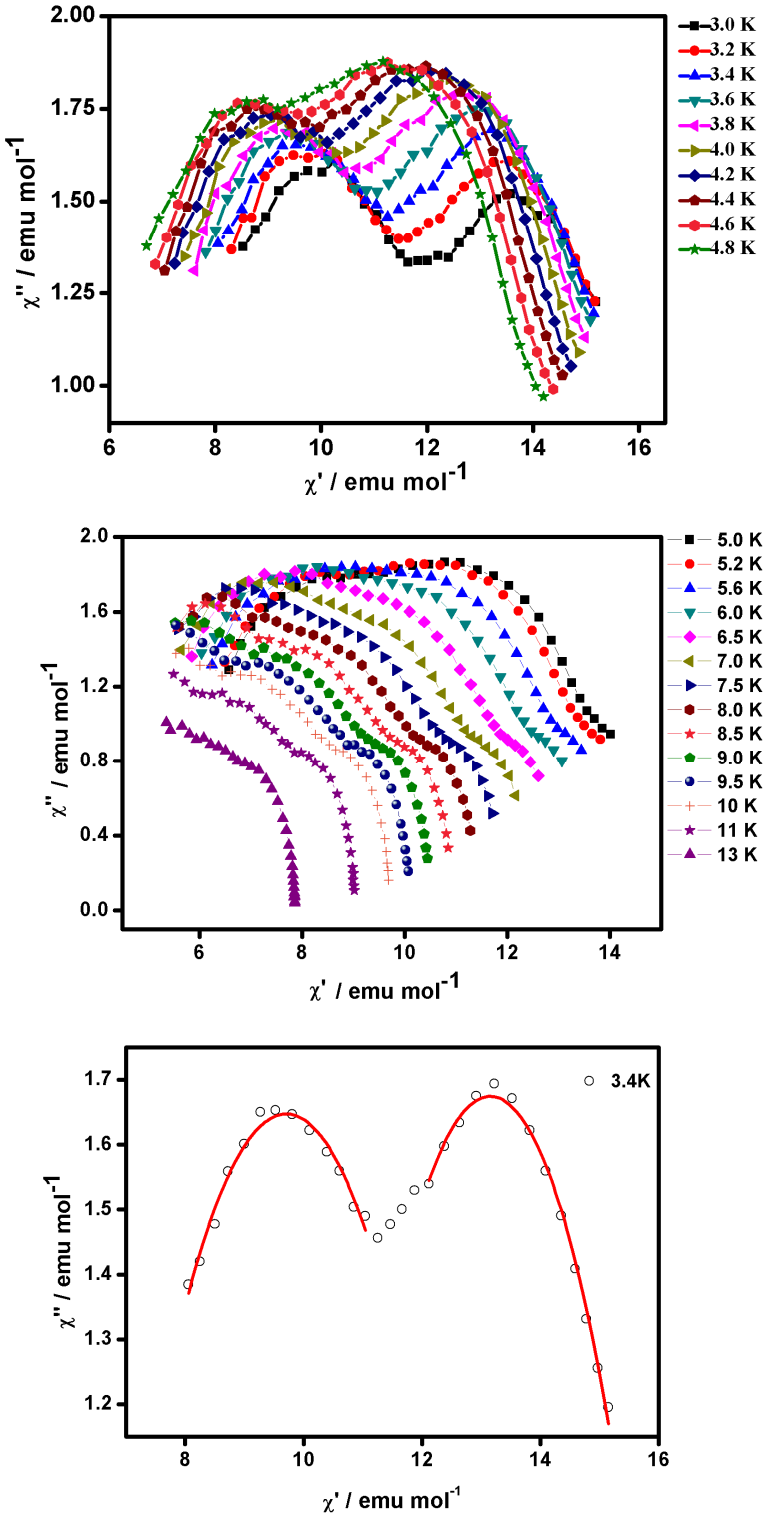

Fig. S10 The Cole-Cole plots of **Dy_3L**. Solid lines are eye guides. The red lines are the best fitting.

Table S6 The parameters of the Cole-Cole plots fitted by the general Debye models.

T / K	FR			SR		
	χ_0	χ_1	α_1	χ_3	χ_4	α_2
2.6	7.01	13.89	0.47	10.47	17.76	0.57
2.8	6.45	13.86	0.49	10.46	17.21	0.50
3.0	6.34	13.66	0.48	10.28	16.93	0.46
3.2	6.15	13.54	0.47	9.96	16.76	0.44
3.4	5.97	13.45	0.47	9.80	16.50	0.41
3.6	6.00	12.94	0.43	8.98	16.52	0.45
3.8	5.88	12.86	0.42	8.57	16.31	0.45
4.0	5.74	12.65	0.41	8.29	16.06	0.44
4.2	5.64	12.50	0.40	8.07	15.80	0.43
4.4	5.65	11.98	0.36	7.64	15.61	0.44
4.6	5.46	12.03	0.37	7.19	15.42	0.46
4.8	4.60	13.20	0.50	6.74	15.22	0.47
5.0	4.88	12.59	0.44	6.09	15.06	0.50
5.2	4.92	12.08	0.40	6.14	14.58	0.47
5.6	5.12	10.50	0.26	4.45	14.43	0.54
6.0	4.08	12.47	0.47	5.88	13.46	0.44

3. Ferroelectric properties

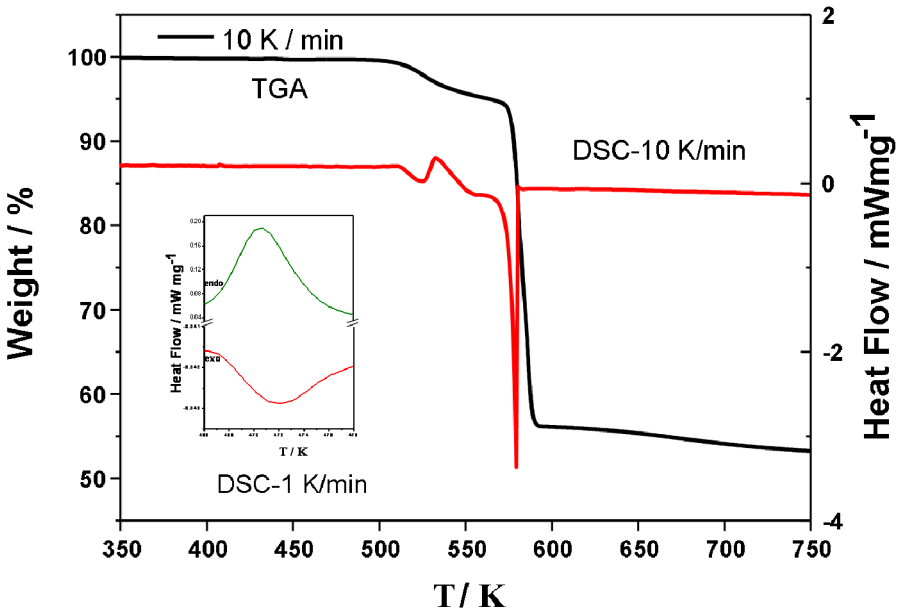

Fig. S11 The TGA and DSC curves of **Dy_3L**. The red and green (inset) lines are measured in the heating rate of 10 K/min and 1 K/min, respectively.

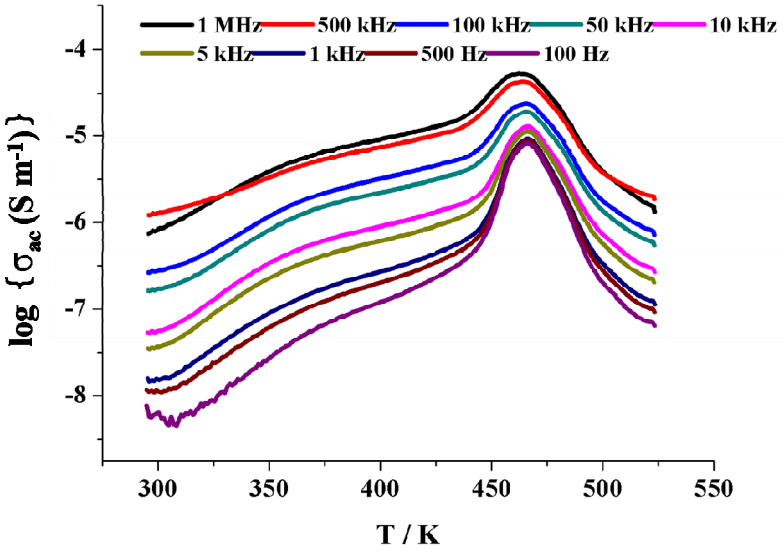

Fig. S12 Temperature-dependent ac conductivities of **Dy_3L**

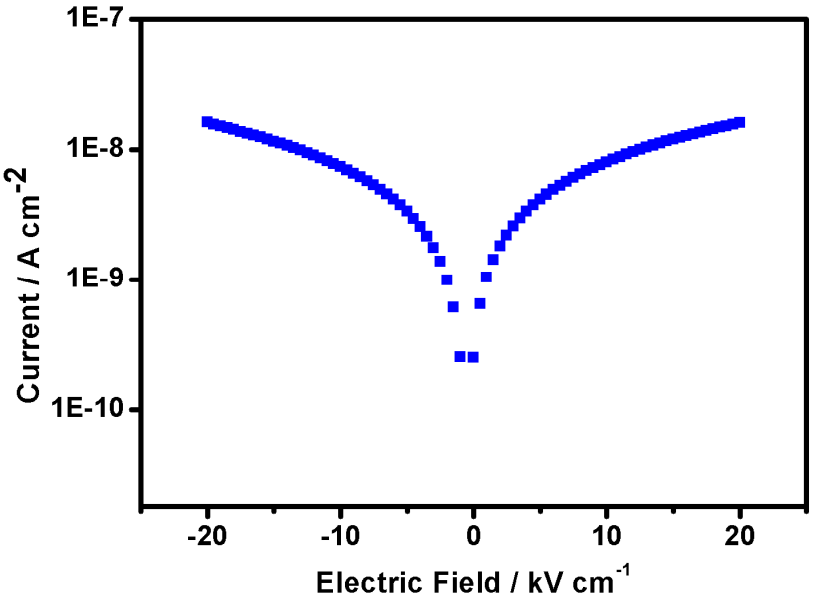

Fig. S13 The plot of the leakage currents versus electric fields of **Dy_3L**.

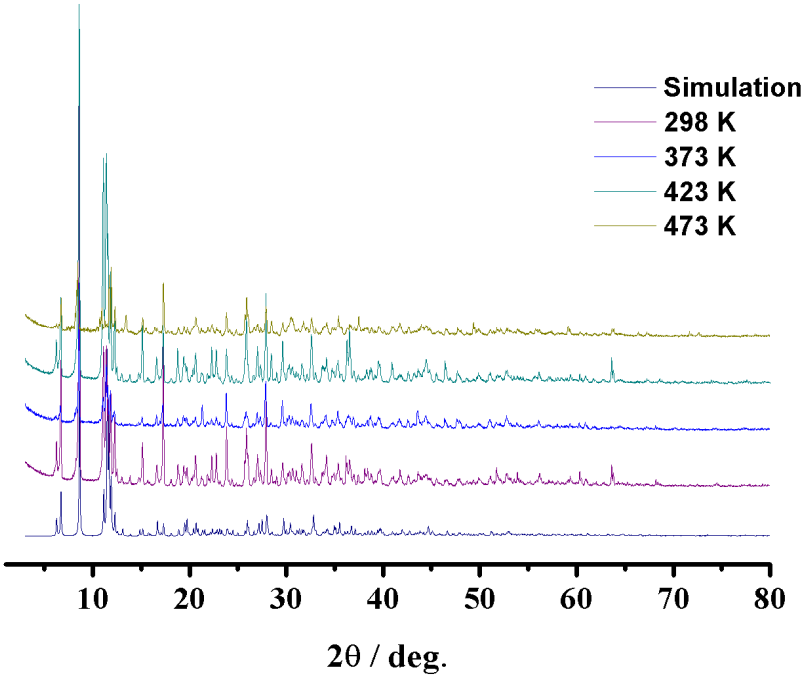

Fig. S14 Powder X-ray diffraction patterns of **Dy_3L**.

4. References

1. G. Sheldrick, *Acta Crystallogr. A,* 2008, **64**, 112.
2. F. Aquilante, L. De Vico, N. Ferre, G. Ghigo, P. A. Malmqvist, P. Neograd y, T. B. Pedersen, M. Pitonak, M. Reiher, B. O. Roos, L. Serrano-Andres, M. Urban, V. Veryazov and R. Lindh, *J. Comput. Chem.,* 2010, **31**, 224-247.
3. L. F. Chibotaru, L. Ungur, C. Aronica, H. Elmoll, G. Pilet and D. Luneau, *J. Am. Chem. Soc.,* 2008, **130**, 12445-12455.
4. L. Ungur, W. Van den Heuvel and L. F. Chibotaru, *New J. Chem.,* 2009, **33**, 1224-1230.